

Fast characterization of carbon/epoxy rings for use in the ball-joints of the Maeslant storm surge barrier

W. Van Paepegem^{a,*}, L. Van Schepdael^b, J. Degrieck^a, P. Samyn^a,
P. De Baets^a, E. Suister^c, J.S. Leendertz^c

^a *Department of Mechanical Construction and Production, Ghent University, Sint-Pietersnieuwstraat 41, 9000 Gent, Belgium*

^b *SOLICO BV, Solutions in Composites, The Netherlands*

^c *Ministry of Transport, Public Works and Water Management, The Netherlands*

Available online 28 November 2005

Abstract

In 2004, the rehabilitation works of the Maeslant storm surge barrier in The Netherlands were finished. The two gates of the barrier are attached to a pivotal point on both banks. The pivotal points are designed as two large ball-joints (10 m diameter) that must allow for both horizontal and vertical movements of the gates. Five hundred individual composite material discs provide a low friction sliding contact with the ball.

The composite material consists of a ultra-high molecular weight polyethylene disc, reinforced by a filament-wound carbon/epoxy ring. In this paper, the characterization and qualification tests for the carbon/epoxy rings are discussed. The design of the tests and their numerical validation is presented. It is shown that this combined numerical/experimental approach is essential to obtain reliable results. © 2005 Elsevier Ltd. All rights reserved.

Keywords: Fibre-reinforced composites; Surge barrier; Finite elements; Filament winding; Transverse shear strength

1. Introduction

The south-west part of The Netherlands is located in a low-lying delta, where the Rhine and IJssel rivers run into the North Sea. In 1953, the fatal combination of a north-western storm and spring tide resulted in the inundation of large parts of the provinces of Zeeland and South Holland. In order to prevent a repetition of the disaster, a set of measures were laid down in the Delta Act. Large primary dams were constructed and dikes were elevated. As the seaports of Rotterdam and Antwerp had to remain accessible, no dams could be built in the New Waterway and the Western Scheldt. The elevation of the dikes was not an option as well. Finally, in the 1980s, a movable storm surge barrier appeared to be the most attractive in terms of cost, environmental effects and safety [1].

This Maeslant storm surge barrier consists of two hollow semi-circular gates attached by means of steel arms to a pivotal point on both banks, as illustrated in Fig. 1. In the event of a storm tide, the “parking” docks are filled with water, so that the hollow gates start to float and can be turned into the New Waterway. Once the gates meet, the cavities are filled with water and the gates sink to the bottom, thus sealing off the 360 m wide opening.

The two ball-joints are designed to ensure that the gates can move in all directions, both horizontally (when the gates are turned into the waterway) and vertically (upon submersion). With a diameter of 10 m and a weight of 680 tons, the ball-joints are more than three times as big as the largest ball-joint ever used. In the front, rear and bottom pedestals of the ball-joints, 500 machined holes provide place for the composite material discs that must guarantee low friction sliding contacts at high normal pressures (up to 150 MPa), as illustrated in Fig. 2.

In this paper, the characterization tests for the composite material discs are discussed. First the general design of

* Corresponding author.

E-mail address: Wim.VanPaepegem@UGent.be (W. Van Paepegem).



Fig. 1. View on the Maeslant storm surge barrier [1].

the composite material disc is presented. Next the different types of characterization tests are investigated, together with their numerical validation.

2. Design of the composite material disc

The demands for the composite material discs are very high, due to the combination of low friction and very high normal pressures. The design of the composite material disc was done by Solico, Solutions in Composites (The Netherlands). It consists of a central UHMWPE (ultra-high molecular weight polyethylene) disc, reinforced with a carbon/epoxy ring. These composite discs are placed in the 500 machined holes of the ball-joint, as shown in Fig. 3.

The geometry of the composite discs is shown in Fig. 4. The UHMWPE disc consists of an upper and lower part and a filament wound carbon/epoxy ring encloses the polymer disc. An exploded view of the manufactured discs is shown in Fig. 5.

Although the yield stress of the UHMWPE is about 20 MPa, the normal pressure on the composite material discs can reach values of about 150 MPa in normal working conditions, and laboratory tests have been done up to a load carrying capacity of 400 MPa. As the polyethylene has been “locked up” by the carbon/epoxy ring, these high pressures can be attained.

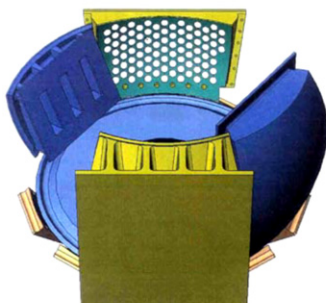


Fig. 2. Top view of the ball-joint (left) and machining of the 500 holes in the pedestals (right) (courtesy of Rijkswaterstaat).



Fig. 3. Positioning of the composite disc in the pedestals of the ball-joint (courtesy of Rijkswaterstaat).

The carbon/epoxy rings were manufactured by filament winding and only unidirectional hoop winding was applied. The qualification tests for these rings were done by Ghent University (Belgium) under the authority of Rijkswaterstaat, the Ministry of Transport, Public Works and Water Management (The Netherlands).

3. Qualification tests for the carbon/epoxy rings

As the carbon/epoxy ring is only reinforced in the hoop winding direction, the composite can be considered transversely isotropic, with five independent elastic constants E_{11} , E_{22} , ν_{12} , ν_{23} and G_{12} . The (tangential) direction \vec{e}_1 is oriented along the reinforcing carbon fibres, \vec{e}_2 is the (radial) direction transverse to the fibres and \vec{e}_3 is the thickness direction, so that $(\vec{e}_1, \vec{e}_2, \vec{e}_3)$ constitute a right-handed coordinate system. The value of the elastic constants is listed in Table 1.

Using 3D (axial load + shear load) non-linear finite element modeling, the stresses in the UHMWPE disc and the composite ring were simulated. The Ultimate Limit State for the most heavily loaded discs in the ball-joint pedestals corresponded with a vertical compressive force of -8000 kN and a shear force of 500 kN. The friction coefficient was determined from a large-scale experimental pro-

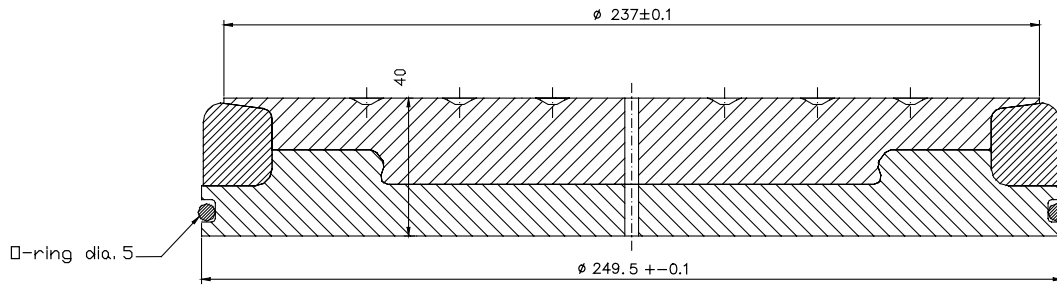


Fig. 4. Geometry of the UHMWPE disc with reinforcing carbon/epoxy ring (courtesy of SOLICO, Solutions in Composites).

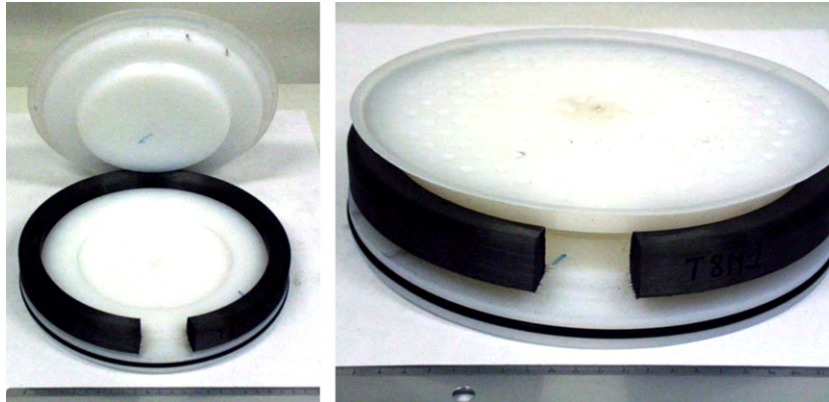


Fig. 5. Exploded view of the UHMWPE disc with reinforcing carbon/epoxy ring.

Table 1
Value of the elastic constants of the carbon/epoxy ring

E_{11}	150 GPa
$E_{22} = E_{33}$	9 GPa
$\nu_{12} = \nu_{13}$	0.34
ν_{23}	0.5
$G_{12} = G_{13}$	4 GPa
G_{23}	3 GPa

gram [2], being 0.0625 in this case. The corresponding 3D finite element mesh is illustrated in Fig. 6.

This combined normal and shear loading leads to a complex stress state in the filament wound ring. The carbon/epoxy ring must withstand (i) high tensile hoop stresses σ_{11} , (ii) radial compressive stresses σ_{22} , (iii) high compressive stresses σ_{33} and (iv) transverse shear stresses τ_{23} . The stress distributions for σ_{11} , σ_{22} , σ_{33} and τ_{23} are shown in Figs. 7–10, respectively.

The safety factor on fibre fracture (catastrophic failure) is in all cases larger than 2.0. For the ULS condition, the maximum stress σ_{11} is 1094 MPa, while the failure stress is larger than 2450 MPa.

The most critical stress is the transverse shear stress τ_{23} . In the areas where no compressive stresses σ_{22} and σ_{33} are present, the transverse shear stress τ_{23} has values up to about 20 MPa, while in the area where compressive stresses σ_{22} and σ_{33} are present, the transverse shear stress τ_{23} reaches values of more than 80 MPa.

Therefore, the experimental tests should allow for a reproducible characterization of the shear strength of

the carbon/epoxy ring transverse to the fibre direction. Several tests were performed, with varying geometry and test parameters. Three main tests can be distinguished:

- *Determination of the fibre volume content by matrix digestion.* The fibre volume fraction V_f of the carbon/epoxy rings must be limited, because it is well-known

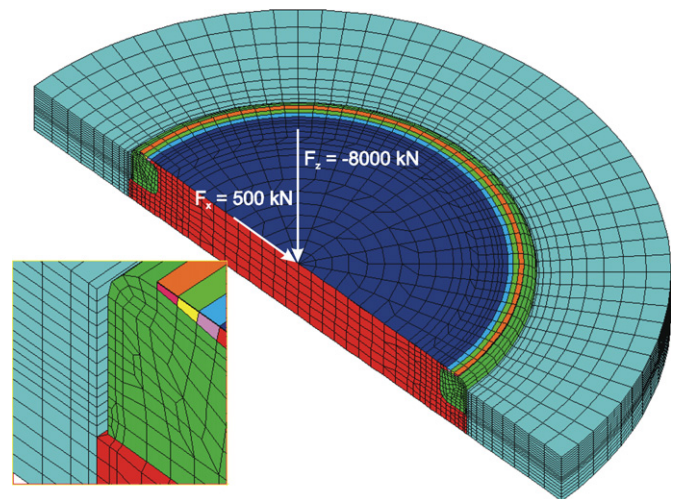


Fig. 6. 3D finite element mesh of the assembly of the UHMWPE disc and the carbon/epoxy ring in one of the machined holes of the pedestal (courtesy of SOLICO, Solutions in Composites).

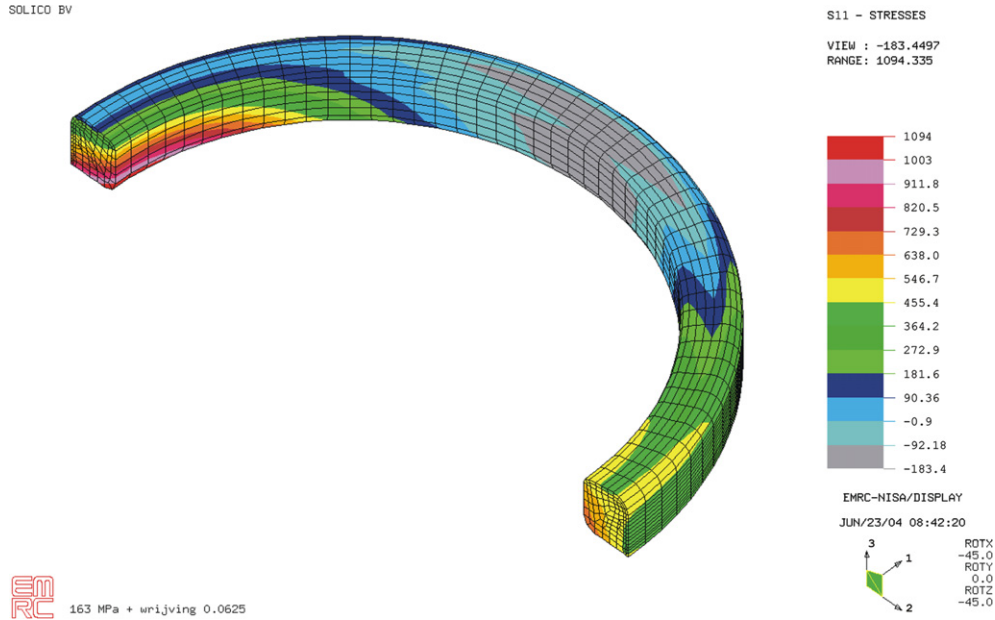


Fig. 7. Distribution of hoop stress σ_{11} along the fibre direction (courtesy of SOLICO, Solutions in Composites).

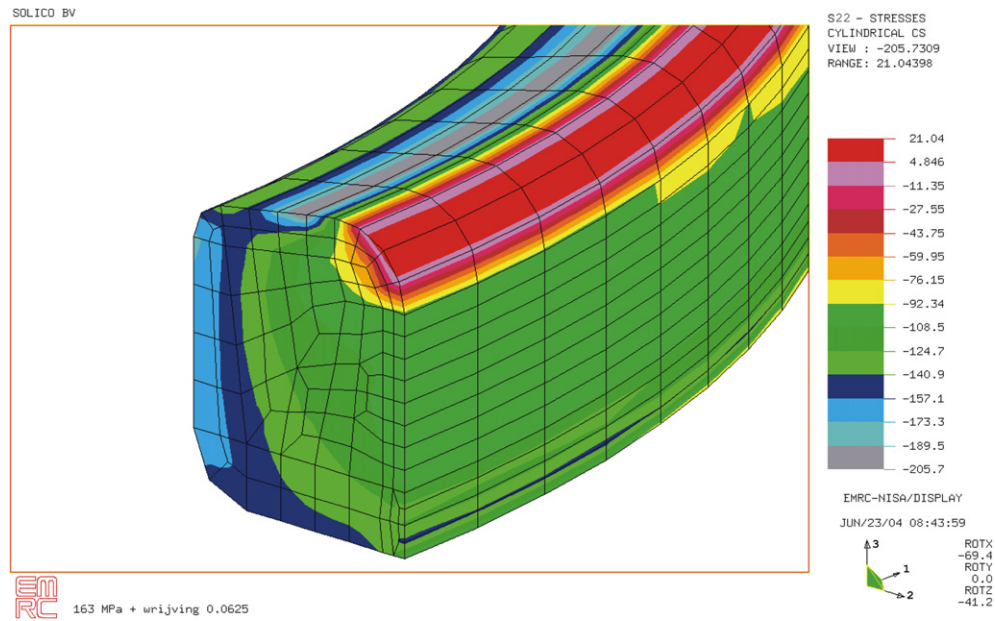


Fig. 8. Distribution of radial stress σ_{22} transverse to the fibre direction (courtesy of SOLICO, Solutions in Composites).

that too high fibre volume fractions result in high stress concentrations in the matrix and thus a lower transverse shear strength overall. In Ref. [3], it can be found that there is a strong relation between the strain magnification in the fibre/matrix interface region and the fibre volume fraction.

- *Compression tests.* These tests were done to evaluate the transverse shear strength.
- *Short-beam tests.* By using the short-beam test, the apparent interlaminar shear strength can be tested. It is a good indicator for the quality of the composite and the resistance against delamination.

3.1. Fibre volume content

The fibre volume content was to stay below 63%. The fibre volume content was determined in accordance with two different international standards: (i) ISO 11667:1997 Fibre-reinforced plastics—Moulding compounds and pre-pregs—Determination of resin, reinforced-fibre and mineral-filler content—Dissolution methods, and (ii) ASTM D3171-99 Standard test methods for constituent content of composite materials. After comparison, the ASTM D3171-99 standard was retained, where the epoxy matrix digestion is done in 70% nitric acid.

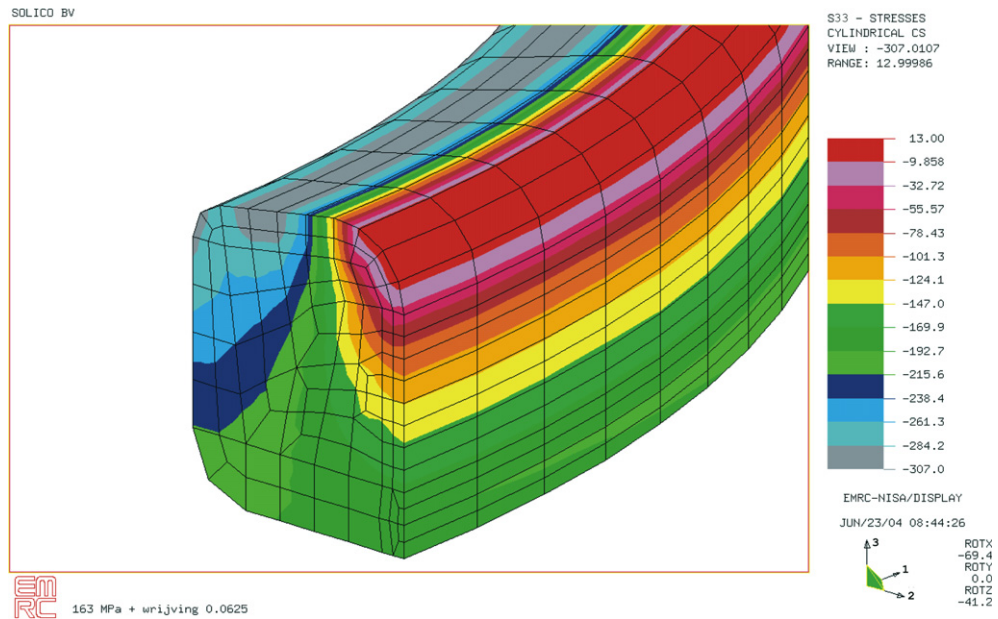


Fig. 9. Distribution of through-the-thickness stresses σ_{33} (courtesy of SOLICO, Solutions in Composites).

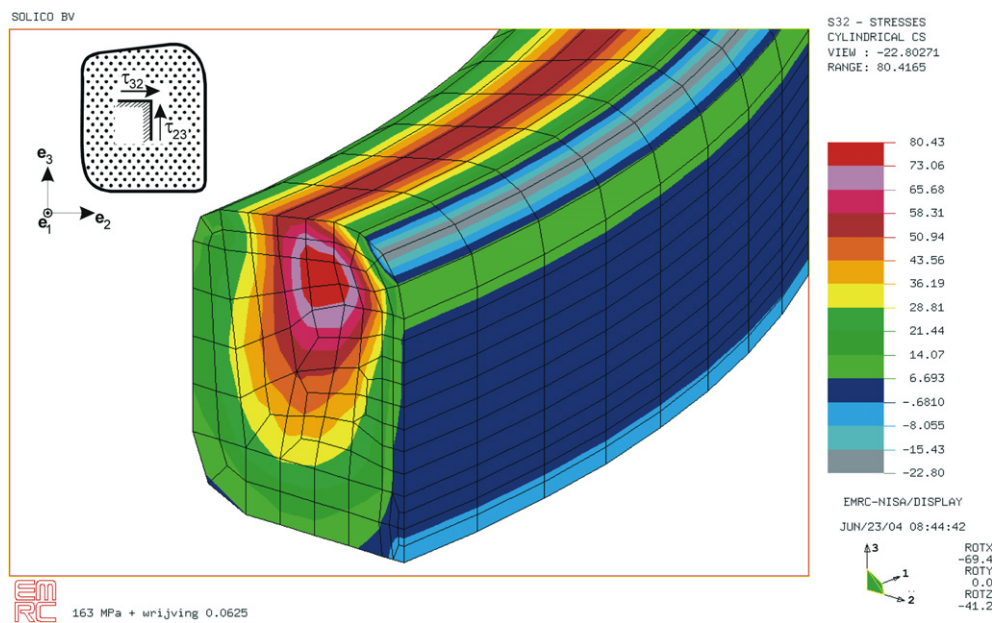


Fig. 10. Distribution of transverse shear stresses τ_{23} (courtesy of SOLICO, Solutions in Composites).

These tests are expensive, due to the long duration of the test. Although all tested matrix systems were epoxies, the difference in digestion time could significantly differ. For some types of epoxy matrix, undigested matrix parts remained after 5 h digestion time (see Fig. 11) and needed two additional runs before results converged to a stable value.

The calculation of the void content strongly depends on the volumic mass of the epoxy matrix. It appeared that it is recommended to measure this volumic mass experimentally, as it can depend on the parameters of the filament winding process.

As it is likely that too high fibre volume contents will lead to poor shear behaviour (due to the stress concentrations in the matrix), faster qualification tests were sought. The first one was a compression test.

3.2. Compression tests

Compression tests on a segment of the carbon/epoxy rings would be difficult to interpret, due to the non-rectangular shape of the cross-section (see Fig. 4) and the curved length. Therefore small bricks were cut out of the carbon/epoxy rings and tested between two compression plates. In



Fig. 11. Undigested epoxy matrix parts after 5 h digestion time.

Table 2
Experimentally measured compressive strength

Sample	Area (mm ²)	Max. force (kN)	σ_{\max} (MPa)
B37X-1	203.82	21.200	104.015
B37X-2	200.88	20.946	104.272
B37X-3	202.96	19.858	97.844

strength. Finite element simulations were done by Solico, Solutions in Composites (The Netherlands) and learned that friction at the surface of the two compression plates was very important. Fig. 14 shows the calculated principal shear stress distribution in the composite specimen. Only a quarter of the specimen was modelled, due to symmetry conditions, and the compressive force was applied to the top surface of the specimen.

If no lateral contraction of the top surface of the specimen is allowed (friction with compression plates), very high shear stresses appear at the corners of the specimen. In the centre of the specimen, the critical shear stress is about 46 MPa, corresponding very well with half the measured compressive strength.

It is important to stress the fact that no stress–strain curves can be directly deduced from the experimental data. In compression tests, the assumption of the infinite rigidity of the machine assembly compared to the specimen’s stiffness is not always valid, and displacement data of the machine cannot be related to compressive strains right away. To that purpose, the displacement between the compression plates must be measured separately (for example by LVDT’s).

order to guarantee the perfect alignment of the gravity center of the composite specimen and the machine plates, a separate disc with a central opening was clamped over the lower compression plate. The set-up is shown in Fig. 12.

Fig. 13 shows the typical fracture surface of the failed specimens. The specimens clearly fail in shear mode, although the shear angle is not 45°, but steeper.

Table 2 shows the experimentally measured compressive strength for three specimens from the filament wound carbon/epoxy ring. The average compressive strength was 102.04 MPa.

A combined numerical/experimental approach appeared necessary to make an estimate of the corresponding shear

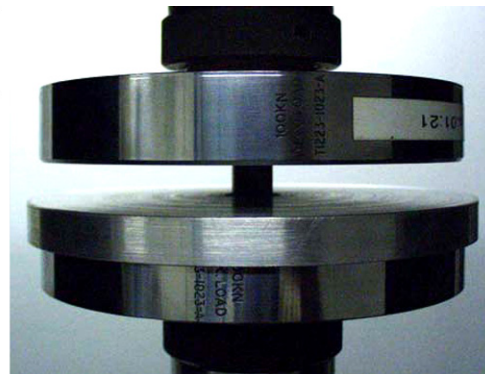
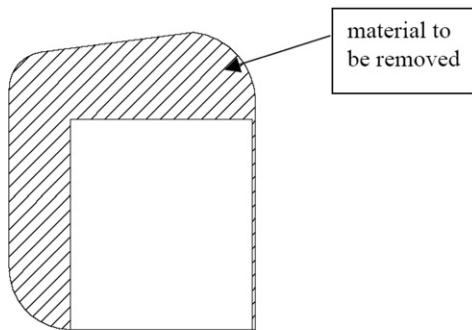


Fig. 12. Compression test on the composite specimens: geometry of the specimen (left) and test set-up (right).

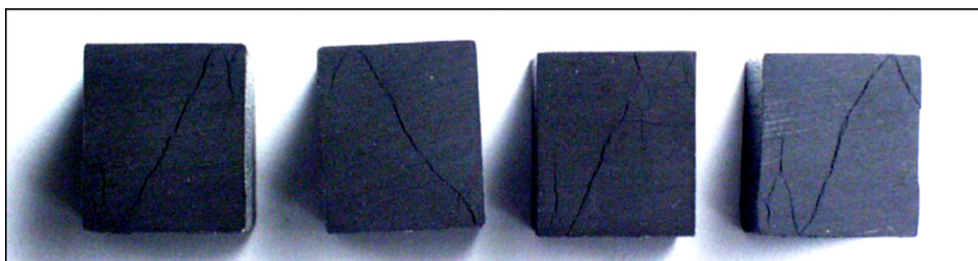


Fig. 13. Fracture surface of the failed specimen.

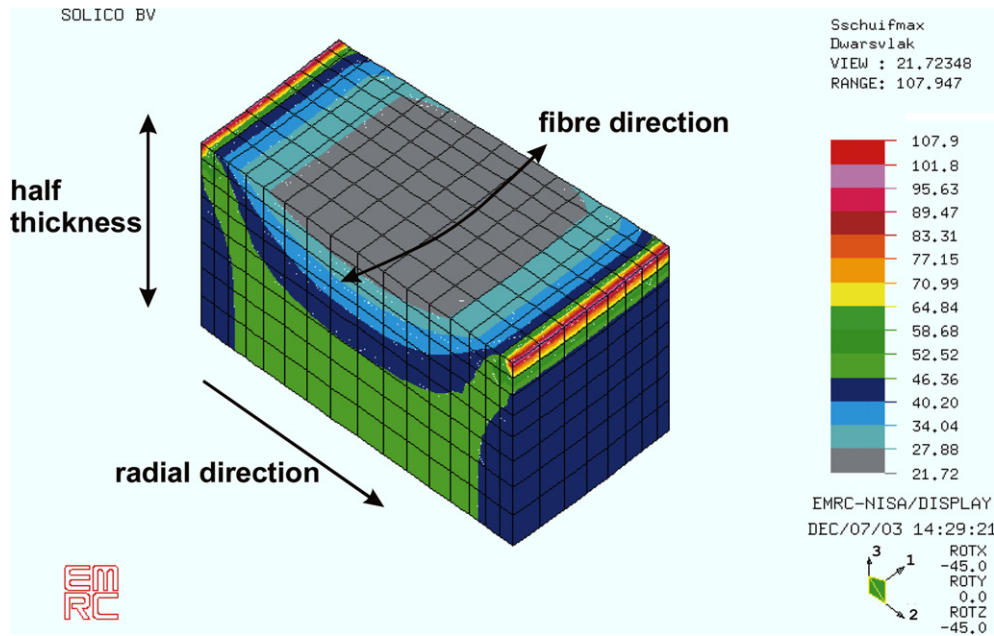


Fig. 14. Finite element calculation of the principal shear stress distribution in the composite specimen (courtesy of SOLICO, Solutions in Composites).

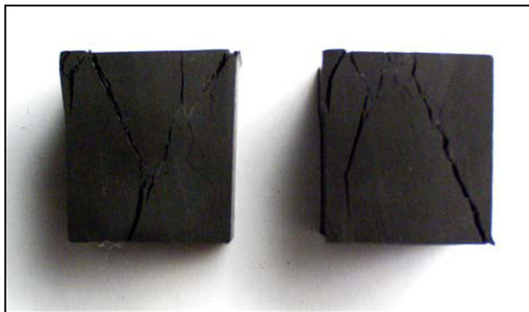


Fig. 15. Fracture surface of full-size composite specimens after compressive failure.

Due to the high cost of machining the specimen to the exact geometric shape, the compression test was given up. Nevertheless, it is worthwhile to mention that compression tests on larger curved ring segments with rectangular cross-section (about 15 mm in width) yielded very comparable results for the transverse shear strength. Also the damage patterns were the same, as illustrated by Fig. 15.

3.3. Short-beam tests

The apparent interlaminar shear strength (ILSS) can be measured by using a short-beam three-point bending test. Two standards are applicable: (i) ISO 14130:1997 Fibre-reinforced plastic composites—Determination of apparent interlaminar shear strength by short-beam method and (ii) ASTM D2344/D2344M-00e1 Standard Test Method for Short-Beam Strength of Polymer Matrix Composite Materials and Their Laminates.

The ASTM standard limits the thickness of the segments cut from a ring-type specimen to 6.5 mm, while the carbon/epoxy rings in this case have a nominal radial thickness of 20.0 mm. Reducing the radial thickness to 6.5 mm would require again machining of the specimen, therefore the full thickness of 20.0 mm was retained and finite element simulations were done to assess the effect. The span length was 80.0 mm which corresponds to a recommended span-thickness ratio of 4.

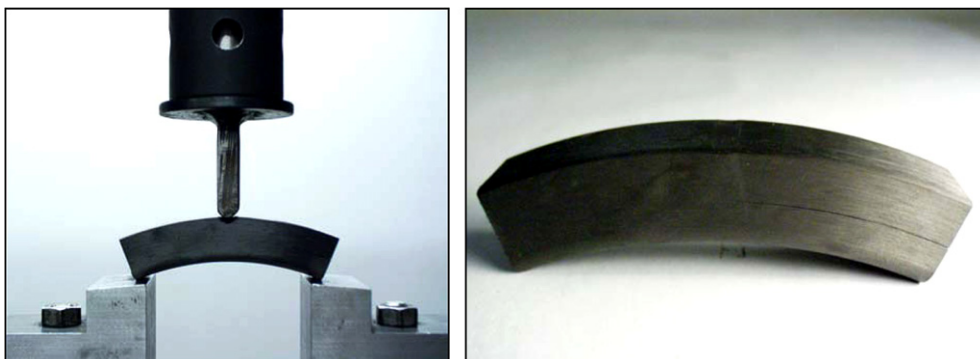


Fig. 16. Experimental set-up for the short-beam test.

Due to the large thickness of the rings and the small radius (compared to the prescribed radius in the ASTM standard), the specimens did not fit on the circular supports. Therefore segments of the carbon/epoxy rings were tested as shown in Fig. 16.

Although this short-beam test was very easy to perform and appeared to be very reproducible, the apparent interlaminar shear stress τ_{12} does not correspond to the transverse shear strength τ_{23} which was calculated in Fig. 10. This is clearly illustrated in Fig. 17.

However, from a comparison between the compression tests and the short-beam tests, it appeared that the ratio between the measured strengths for the transverse shear strength τ_{23} and the apparent interlaminar shear strength τ_{12} was reasonably constant, so that the short-beam test was accepted as a representative qualification test for the shear strength of the filament wound carbon/epoxy rings.

According to the ASTM standard, the apparent interlaminar shear strength is calculated as

$$\tau_{12} = \frac{3}{4} \cdot \frac{F_{\max}}{b \cdot d} \quad (1)$$

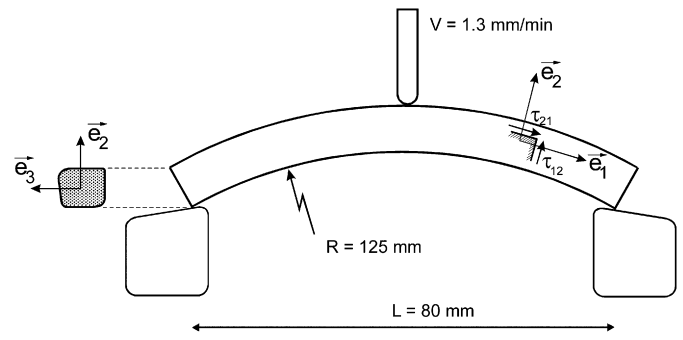


Fig. 17. Definition of the apparent interlaminar shear strength τ_{12} .

where F_{\max} is the maximum force in the short-beam test, and b and d are the width and thickness of the specimen, respectively.

Because the dimensions of the specimens and the test set-up did not comply completely with the international standards, a combined experimental/numerical approach was applied again to interpret the results of the tests. Fig. 18 shows the calculated shear stress distribution in a quarter of the short-beam for a maximum force of

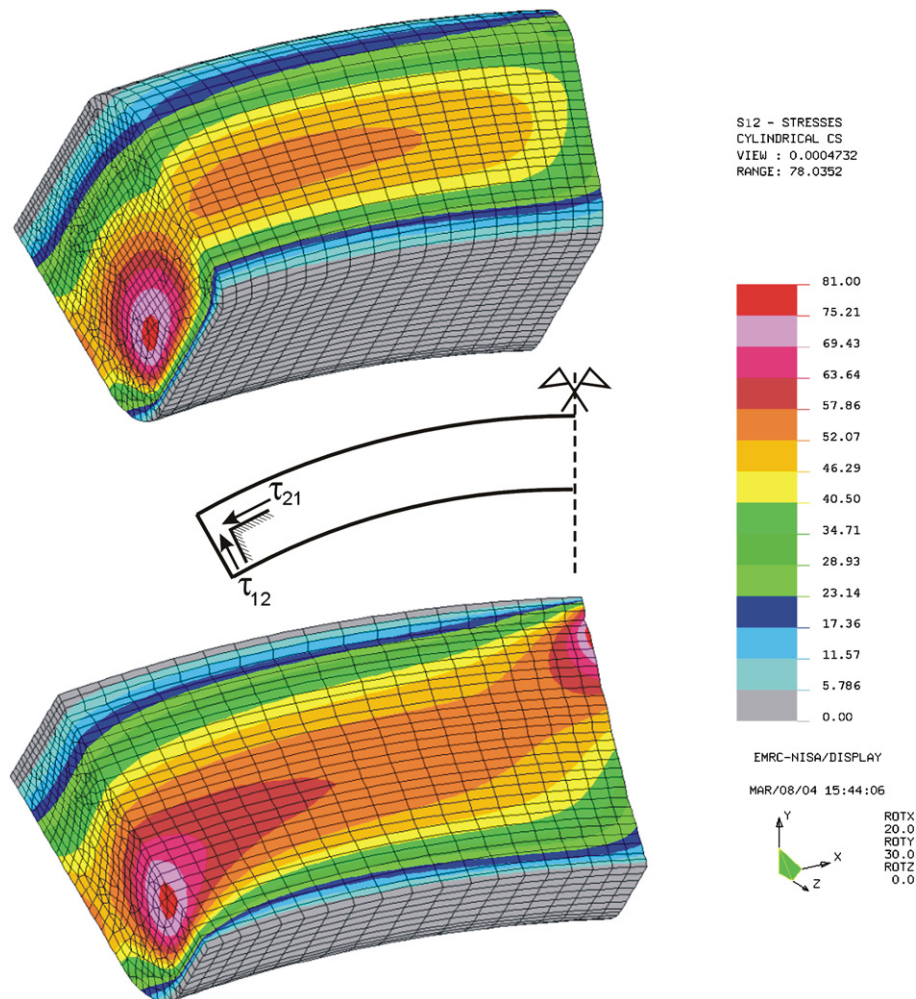


Fig. 18. Finite element simulation of the shear stress in the short-beam specimen (courtesy of SOLICO, Solutions in Composites).

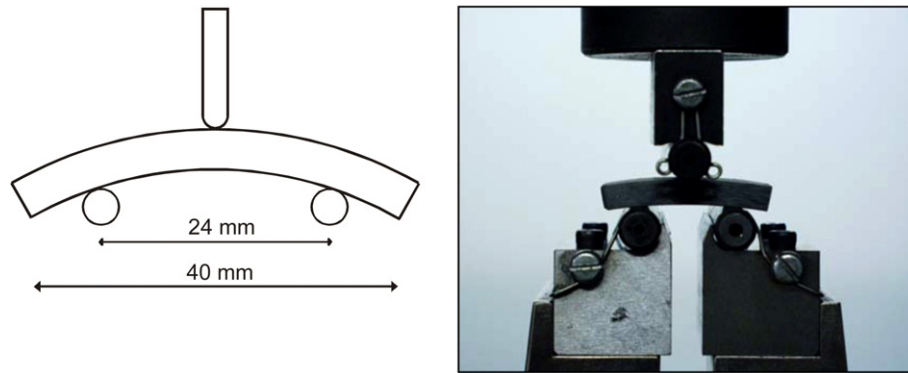


Fig. 19. Experimental set-up for the short-beam test with reduced thickness of the carbon/epoxy specimen.

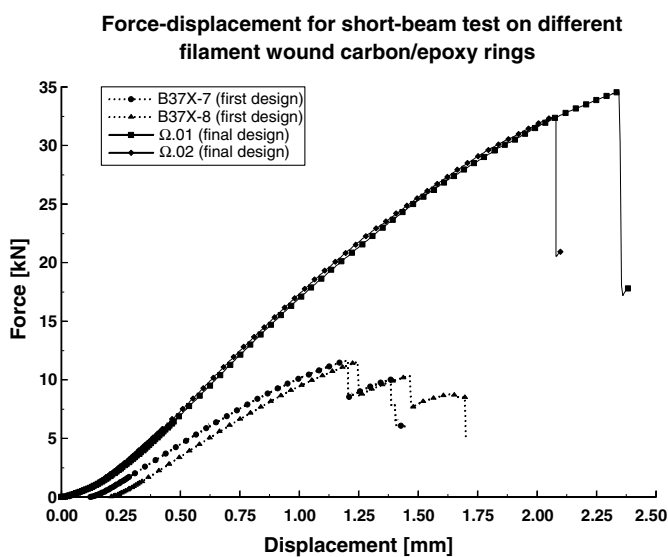


Fig. 20. Experimental results for the short-beam test.

37 kN. The corresponding apparent interlaminar shear strength is 61.3 MPa (Eq. (1)).

The finite element simulations show high stress concentrations at the supports and the load striking edge, but the value in between corresponds reasonably well with the ASTM value.

To validate the results, a few specimens were tested with a reduced thickness of 6.0 mm, in agreement with the ASTM-standard. The span was adjusted in order to obtain the same span-thickness ratio of 4. The test set-up is shown in Fig. 19. It appeared that the measured apparent interlaminar shear strength of 58.8 MPa was in good agreement with the numerically simulated value of about 62 MPa.

The short-beam tests were used during the whole certification process of the filament wound carbon/epoxy rings. The adequate selection of the constituent materials (carbon fibre and epoxy matrix) and the optimization of the filament winding process finally resulted in failure loads for the short-beam tests, that were three times higher than the initial ones. Fig. 20 shows the force–displacement curve

for two samples of the initial design and two samples of the final design.

4. Conclusions

In this paper, the design of composite material discs for use in an extremely high-loaded ball-joint was presented. The discussion focussed on the qualification tests for the carbon/epoxy rings. It was shown that a combined numerical/experimental approach is required, because sole application of internationally standardized test methods does not provide all necessary information.

The main concern in this design was the transverse shear strength of the filament wound carbon/epoxy rings. Three types of tests were distinguished: (i) determination of the fibre volume content by matrix digestion, (ii) compression tests, and (iii) short-beam tests. Careful interpretation of the experimental results, together with finite element simulations, lead to reliable estimates of the composite material properties that are vital for its performance in the Maeslant storm surge barrier.

In September 2004, a successful test closing of the storm surge barrier was performed and inspections afterwards revealed not any occurrence of damage.

Acknowledgements

The author W. Van Paepegem gratefully acknowledges his finance through a grant of the Fund for Scientific Research—Flanders (FWO).

The authors also express their gratitude to SOLICO BV, Solutions in Composites and the Ministry of Transport, Public Works and Water Management in The Netherlands.

References

- [1] Official English website of the Maeslant storm surge barrier in the Netherlands: <http://www.keringhuis.nl/engels/keringhuis/index.html>.
- [2] Leendertz H, Van Schepdael L, Van Paepegem W, Samyn P, De Baets P, Degrieck J. Modification of the ball bearing of the storm surge barrier near Rotterdam (NL). *Stahlbau* 2006;75(1).
- [3] Hull D, Clyne TW. An introduction to composite materials. Cambridge University Press; 1996, ISBN 0 521 28392 2.